XPS and TEM Studies on the Role of the Support and Alkali Promoter in Ru/MgO and Ru−Cs+/MgO Catalysts for Ammonia Synthesis

ARTICLE *in* THE JOURNAL OF PHYSICAL CHEMISTRY C · JUNE 2007

Impact Factor: 4.77 · DOI: 10.1021/jp066970b

7 AUTHORS, INCLUDING:

Yurii V. Larichev
Boreskov Institute of Catalysis
24 PUBLICATIONS **196** CITATIONS
SEE PROFILE

Elena Kalyuzhnaya
Russian Academy of Sciences
14 PUBLICATIONS **107** CITATIONS
SEE PROFILE

Valerii Bukhtiyarov
Boreskov Institute of Catalysis
184 PUBLICATIONS **2,673** CITATIONS
SEE PROFILE

XPS and TEM Studies on the Role of the Support and Alkali Promoter in Ru/MgO and Ru−Cs^+/MgO Catalysts for Ammonia Synthesis

Yurii V. Larichev,[†] Boris L. Moroz,*[,†] Vladimir I. Zaikovskii,[†] Safar M. Yunusov,[‡] Elena S. Kalyuzhnaya,[‡] Vladimir B. Shur,[‡] and Valerii I. Bukhtiyarov[†]

G.K. Boreskov Institute of Catalysis, Siberian Branch of Russian Academy of Sciences, 5, Avenue Akademika Lavrentieva, 630090 Novosibirsk, Russia, and A.N. Nesmeyanov Institute of Organoelement Compounds, Russian Academy of Sciences, 28, Vavilova Street, 117813 Moscow, Russia

Received: October 24, 2006; In Final Form: February 6, 2007

The chemical state of ruthenium in the Ru/MgO and Ru−Cs^+/MgO catalysts prepared by the incipient wetness technique with the use of $Ru(OH)Cl_3$ and Cs_2CO_3 as the catalyst and promoter precursors, respectively, is characterized by X-ray photoelectron spectroscopy (XPS). The influence of the final state effects (the differential charging and variations of the relaxation energy) on the binding energy of Ru $3d_{5/2}$ core level measured for supported Ru nanoparticles is estimated by comparison of the Fermi levels and the modified Auger parameters determined for the Ru/MgO and Ru−Cs^+/MgO catalysts with the corresponding characteristics of polycrystalline Ru foil. High-resolution transmission electron microscopy (HRTEM) in combination with energy dispersive X-ray (EDX) microanalysis reveals that Ru particles in the Ru−Cs^+/MgO catalyst are covered with an amorphous layer containing cesium. XPS data show that the layer subjected to the prolonged treatment with H_2 at 450 °C consists of cesium suboxide $Cs_{2+X}O$. The shift of the Ru $3d_{5/2}$ binding energy toward lower values is found for the Ru−Cs^+/MgO catalyst (279.7 eV) with respect to metallic Ru (280.2 eV) and the Ru/MgO catalyst (280.5 eV). It is assumed that the shift results from a decrease in the work function of ruthenium under the action of Cs^+ cations located on the Ru surface. The data obtained are used to explain the sharp difference in the activities of the Ru/MgO and Ru−Cs^+/MgO catalysts for ammonia synthesis at 250−400 °C.

Introduction

In industry, most ammonia is produced from hydrogen and nitrogen via the Haber−Bosch process at high temperatures (425−600 °C) and pressures (20−30 MPa) with fused magnetite-based catalysts.[1] At the same time, a search for more active catalytic systems that allow for operation at milder conditions is in progress. Supported catalysts containing metallic ruthenium particles promise to be the next-generation catalysts for ammonia synthesis.[2−5] It has been stated[6−10] that the type of support greatly influences the catalytic activity of Ru particles: basic supports generally lead to more active catalysts than acidic ones. For example, the metal catalysts prepared from Ru carbonyls and supported on MgO show considerable activity toward ammonia synthesis at the temperature as low as 300−400 °C and under the pressure of an N_2/H_2 mixture close to ambient.[7,9] The substitution of more commercially feasible materials such as alumina or carbon supports for MgO results in a sharp decrease in the catalytic activity of the supported Ru particles. The similar observations led the authors[7,9] to the conclusion that the stronger the support basicity is, the higher the catalytic activity is.

The addition of a basic promoter, e.g., alkali metal oxide or hydroxide, to the Ru/MgO catalyst results in further improvement in its activity for ammonia synthesis.[6,7,11,12] The rate of NH_3 synthesis over the promoted Ru-M^+/MgO catalysts increases depending on the promoter in the following order: $M^+ = Na^+ < K^+ < Rb^+ < Cs^+$, i.e., the catalyst activity increases with a decrease in the promoter electronegativity.

Commonly, the promoting effect of basic supports or promoters on the activity of ruthenium catalysts for ammonia synthesis is explained by their ability to donate electrons to the surface Ru metal atoms.[13−16] Upon adsorption of dinitrogen on the surface of Ru crystallites, the excess electron density is transferred from the d orbitals of Ru atoms to the antibonding orbitals of N_2 molecules. This transfer weakens the N−N bonds and thereby facilitates the dissociation of dinitrogen, which is generally accepted to be the rate-determining step of ammonia synthesis.

Originally, this assumption was based on the results of X-ray photoelectron spectroscopy (XPS) measurements.[6] For Ru/MgO and Ru/CaO catalysts prepared by impregnation of the support with a solution of $RuCl_3$ and reduced with dihydrogen at 475 °C, the binding energy (E_b) of the Ru $3d_{5/2}$ core level was 279.8 and 279.5 eV, respectively. Both E_b values are lower than that observed for bulk Ru metal (280.0 eV). In contrast, the E_b(Ru $3d_{5/2}$) values determined for Ru/Al_2O_3 and Ru/SiO_2 samples prepared the same way were either identical to or even slightly higher than the corresponding value for bulk metallic ruthenium.[6,17] It was found later[11] that the impregnation of the Ru/MgO catalyst with an aqueous $CsNO_3$ solution followed by the treatment with a N_2/H_2 mixture at 101 kPa and 400 °C resulted in the shift of Ru $3d_{5/2}$ and Ru $3d_{3/2}$ peaks by ca. 1 eV to lower E_b with respect to the corresponding peaks of bulk Ru metal. These data were considered evidence for the electron transfer from basic sites of the support and/or promoter to

* Corresponding author. E-mail: moroz@catalysis.nsk.su. Tel: (+7-383)-3397353. Fax: (+7-383)-3308056.
[†] Boreskov Institute of Catalysis.
[‡] Nesmeyanov Institute of Organoelement Compounds.

10.1021/jp066970b CCC: $37.00
Published on Web 06/05/2007

supported Ru metallic particles. Some indirect evidence for the proposition that the basic support and/or promoter donates electrons to surface Ru atoms, facilitating the dissociative adsorption of dinitrogen, has been provided later by examination of Ru/MgO and Ru−M^+/MgO catalysts with alternative research techniques such as Fourier-transform infrared spectroscopy of adsorbed N_2,[14] kinetic isotopic transient analysis,[18,19] and temperature-programmed reaction.[18]

However, it should be kept in mind that, even though the negative shift of the XPS peaks actually can reflect the presence of a negative charge on metal particles due to their interaction with the support or promoter, there may be a number of other factors, including instrumental, which also may cause the shift.[20] Consequently, we believe that the questions regarding whether the charge transfer from basic sites of the support and the promoter to the surface of Ru crystals occurs and what is the reason for the promoting effect of bases on the activity of Ru catalysts for ammonia synthesis are still open. To elucidate the problem, we reexamined the chemical states of ruthenium and cesium in the Ru/MgO and Ru−Cs^+/MgO catalysts by XPS, taking into consideration the so-called "final state effects" appearing as a result of photoelectron emission such as differential charging of the metallic Ru crystallites supported on a dielectric support and the relaxation effect which also may be responsible for the variation of E_b values. In addition, high-resolution transmission electron microscopy (HRTEM) in combination with energy-dispersive X-ray (EDX) microanalysis was applied for studying the location of the Cs promoter on the catalyst surface. On the basis of the data obtained, we suggest an explanation for the promotional effect of cesium in ruthenium-based ammonia synthesis catalysts in terms different from the previous concepts.

Experimental Methods

Preparation of the Support. Magnesia used as the support was prepared by precipitation from an aqueous solution of $Mg(NO_3)_2$ with a KOH solution followed by drying in air. Powdered magnesium hydroxide was pressed into pellets, crushed, and sieved to a particle size of 0.2−0.5 mm, then calcined in flowing dry air at 450 °C for 2 h, and finally, heated in a vacuum at the same temperature for 3 h. Magnesia thus prepared exhibited BET surface area of 200 m^2/g. It was stored under Ar and drawn to air just prior to impregnation with the Ru compound.

Catalyst Preparation. To prepare catalysts, ruthenium and cesium compounds were deposited onto the magnesia surface under anhydrous conditions in order to prevent the support from strong morphological changes caused by the interaction with water and partial conversion of MgO to $Mg(OH)_2$.[21] The support was incipient wetness impregnated with an acetone solution of ruthenium hydroxychloride, $Ru(OH)Cl_3$, containing 44.8 wt.% Ru. Immediately after adding the impregnation solution to the support, the solvent was removed by blowing air through to obtain the dry-air sample. Subsequently, the sample was evacuated at room temperature for 2 h and then at 50 °C for another 2 h. Due to the low solubility of $Ru(OH)Cl_3$ in acetone, the impregnation procedure was repeated twice. After the last portion of $Ru(OH)Cl_3$ was deposited, the sample was evacuated at 50 °C for 6 h, heated in flowing hydrogen to 450 °C for 2.5 h, and reduced under these conditions for another 6 h. After reduction, the Ru/MgO sample (5.0 wt % Ru) was cooled in a H_2 flow to room temperature, transferred from the reactor to a glass ampule without atmospheric exposure, and stored in the ampule filled with argon. The promoter precursor (Cs_2CO_3) was deposited onto the Ru/MgO sample by incipient wetness impregnation from the solution in anhydrous ethanol at 70 °C. The solvent was removed by blowing argon through the sample. The dry-air sample was evacuated at room temperature for 2 h and then at 50 °C for another 2 h. Another three impregnation cycles were conducted because of low solubility of Cs_2CO_3 in anhydrous ethanol. As soon as the impregnation was accomplished, the sample was evacuated at 50 °C for 6 h, heated in flowing hydrogen to 450 °C for 2.5 h, and calcined under these conditions for another 6 h. Subsequently, the Ru−Cs^+/MgO sample (4.5 wt % Ru, 4.5 wt % Cs, Cs/Ru = 0.8 mol/mol) was cooled to room temperature, transferred from the reactor to a glass ampule without atmospheric exposure, and stored in the ampule filled with argon.

As a reference sample, 3.5 wt % Cs^+/MgO was prepared by impregnation of MgO with Cs_2CO_3 by the above-described procedure.

Catalytic Tests. Catalytic ammonia synthesis was carried out in a plug-flow system at 200−400 °C under 101 kPa using a stoichiometric (1:3) N_2/H_2 mixture at a flow rate of 170 mL/min. The reaction feed was deoxidized (to the level <0.1 ppm O_2) and dried (<0.5 ppm H_2O) by passing successively through the columns filled with active alumina, a reduced Ni−Cr catalyst, and molecular sieves NaA and NaX. A weighed catalyst sample (2.0−2.5 g) was transferred to a glass reactor under synthesis gas (1:3 N_2/H_2) atmosphere (without contact with air) and heated to 200 °C. As soon as the outlet NH_3 concentration ceased to change noticeably with time (pseudo-stationary state), the reaction temperature was risen by 50 °C, and the reaction again was carried out until reaching the pseudo-stationary state of the catalyst at the given temperature. For determination of the outlet NH_3 concentration, the gas flow after reactor was passed through an aqueous H_2SO_4 solution of a known concentration, and the time interval needed to neutralize a certain amount of the acid at constant flow rate, temperature, and pressure was measured. The stationary outlet NH_3 concentration was calculated by averaging results of 6 to 10 measurements at identical conditions (the standard deviations from the mean value were within the range 0.002−0.008 vol %). The detection limit of the ammonia concentration was 0.005 vol %.

Methods for Structure and Morphology. X-ray diffraction (XRD) was performed using a HZG-4 X-ray diffractometer with Cu Kα radiation and a graphite monochromator. The data were collected for 5 s per step with a step size of 0.05° within the range $20° \leq 2\theta \leq 90°$. Prior to XRD analysis, a sample was quickly ground in air and wrapped in an organic polymer film, which prevented it partly from contact with air during the XRD pattern measurement.

HRTEM studies were carried out on a JEOL JEM-2010 transmission electron microscope operated at 200 kV and giving an information limit of 0.14 nm. Energy-dispersive X-ray (EDX) analysis of chemical composition of various structural features observed in the materials under study was performed using an EDAX spectrometric unit attached to the same electron microscope and equipped with a Si(Li) detector giving an energy resolution of 130 eV. Just prior to the examination, a sample was taken out from the ampule filled with argon, quickly ground, and suspended in hexane. A drop of suspension was mounted on a copper grid coated with a holey carbon film, and the solvent was allowed to evaporate.

Particle-size distributions of the Ru crystallites were determined from TEM micrographs. No less than 400 crystals were included in the distribution for each sample. High-resolution

TABLE 1: Results of Testing the Ru/MgO and Ru−Cs^+/MgO Catalysts in Ammonia Synthesis[a]

temperature (°C)	stationary NH_3 concentration in the reactor outlet gas (vol %) Ru/MgO	Ru−Cs^+/MgO	equilibrium NH_3 concentration[b] (vol %)
250	<0.005	0.015	5.40
300	<0.005	0.15	2.17
350	<0.005	0.67	0.86
400	<0.005	0.43	0.44

[a] All data were measured at 101 kPa of 1:3 N_2/H_2 gas mixture, total flow rate of 170 mL/min and catalyst weight of ~2.3 g (~1.0 mg-at Ru). [b] The data are taken from ref 23.

imaging was carried out to determine interplanar distances of the Ru crystallites and to elucidate the location of the Cs promoter.

Ruthenium dispersion was determined by CO pulse chemisorption at 25 °C using a He flow of 25 mL/min and pulses of 0.09 mL (10% CO in He) on a Micromeritics AutoChem II 2920 unit. Prior to dispersion analysis, the Ru/MgO and Ru−Cs^+/MgO samples were freshly treated with flowing H_2 (25 mL/min) at 200 °C for 15 min and then flushed with He (25 mL/min). In order to calculate the metal dispersion, the stoichiometry of Ru/CO = 1 was assumed.

X-ray Photoelectron Spectroscopy. X-ray photoelectron (XP) spectra were measured with a VG ESCALAB HP photoelectron spectrometer, using a non-monochromatized Al Kα radiation ($h\nu$ = 1486.6 eV) operated at 200 W as the excitation source. The binding energy scale was calibrated using the peaks of Au $4f_{7/2}$ (E_b = 84.0 eV) and Cu $2p_{3/2}$ (E_b = 932.6 eV) from polycrystalline gold and copper foils, respectively. The charging effect was corrected using the Mg 2s peak from MgO at 88.1 eV as the internal reference. The charging value was determined as the difference between the measured and tabulated E_b(Mg 2s) values.

For XPS study, a sample was pressed into a Ni grid immediately after unsealing the storage ampule and transferred to a preparation chamber of spectrometer (the samples were exposed to air for no more than 5 min during this procedure). In the preparation chamber, the sample usually was re-reduced with H_2 under static conditions at 350 °C and 101 kPa for 1 h, then outgassed to 10^{-5} Pa and transferred into the analyzer chamber. In some cases, the additional hydrogen treatment was not used before recording the spectra. To measure the spectra of polycrystalline ruthenium foil (denoted later as Ru(poly)), the sample was cleaned by the standard high-vacuum procedure including Ar ion sputtering followed by O_2 adsorption at 200 °C and 10 Pa for 10 min and subsequent annealing in vacuum at 700 °C. Cesium was evaporated onto the Ru(poly) surface in the preparation chamber using a getter flash source in vacuum ($P < 5 \times 10^{-7}$ Pa) or in flowing oxygen (P = 0.01 Pa) at room temperature.

The E_b values and the areas of XPS peaks were determined after analysis of the line shapes by curve fitting of the experimental data using Gaussian−Lorentzian functions and Shirley background subtraction. Quantitative analysis was performed from the areas of XPS peaks corrected by the atomic sensitivity factors of the corresponding elements.[22]

Results

Catalytic Activity in Ammonia Synthesis. Table 1 shows results of testing the Ru/MgO and Ru−Cs^+/MgO catalysts in ammonia synthesis at atmospheric pressure. With the Ru/MgO catalyst, the NH_3 concentration in the reactor outlet gas mixture is below the detection limit (<0.005 vol %) over the whole temperature range examined (200−400 °C). At the same time, the formation of NH_3 over the promoted Ru−Cs^+/MgO catalyst is detected at temperature as low as 250 °C. At 350 and 400 °C, the NH_3 outlet concentration reaches 78% and 98% of the corresponding NH_3 equilibrium yields, respectively. It confirms that the activity of the Ru/MgO catalyst in ammonia synthesis is significantly increased due to promotion with cesium (at 300 °C, the promoted catalyst is more active than the nonpromoted catalyst at least by a factor of 30).

TABLE 2: Mean Ru Particle Diameter and Dispersion as Determined by TEM, XRD, and CO Chemisorption[a]

sample	mean particle diameter (nm) $\langle d_l \rangle$	$\langle d_{vs} \rangle$	$\langle d$(XRD)$\rangle$	disp. TEM (%)	disp. CO (%)
Ru/MgO	3.5	8.5	10.0	12.1	11.5
Ru−Cs^+/MgO	3.2	9.8	9.0	10.3	6.2

[a] The values in this table are defined as follows: $\langle d_l \rangle = \Sigma n_i d_i / \Sigma n_i$, $\langle d_{vs} \rangle = \Sigma n_i d_i^3 / \Sigma n_i d_i^2$, where n_i is the number of Ru particles having diameter d_i, which are seen in TEM micrographs. $\langle d$(XRD)$\rangle$ is the Ru crystallite size corresponding to the X-ray Ru(001) reflection calculated by the Scherrer equation: $\langle d(\mathrm{XRD}) \rangle = K\lambda/(b - b_0) \cos\theta$ where λ is wavelength of the X-ray; θ is one-half the scattering angle; b and b_0 are the observed and the instrumental half-widths of the peak on the 2θ scale in radians; K = 1.0. Disp. TEM and disp. CO are the Ru dispersions calculated on the basis of $\langle d_{vs} \rangle$ and CO chemisorption values, respectively, assuming spherical metal particles and the stoichiometry of Ru/CO = 1.[24]

Dispersion of Ru and Location of Cs Promoter. TEM micrographs of the Ru/MgO and Ru−Cs^+/MgO catalysts taken with a medium magnification demonstrate contrast images of spherical Ru particles which are evenly distributed over the support surface. In both samples, the majority of particles are less than 5 nm in diameter (d_i). Besides, few larger Ru particles (d_i = 5−12 nm) are also seen, being in approximately identical number in both samples. Table 2 presents the mean Ru particle diameters ($\langle d_l \rangle$ and $\langle d_{vs} \rangle$) for the Ru/MgO and Ru−Cs^+/MgO catalysts, as determined from particle-size distributions. Both $\langle d_l \rangle$ and $\langle d_{vs} \rangle$ values are similar for the nonpromoted and promoted catalysts (for both catalysts, they fall in the ranges 3.0−3.5 and 8.5−10 nm, respectively). Hence, no considerable changes both in the mean Ru particle size and in the mode of particle-size distribution occur upon promotion of the Ru/MgO catalyst with cesium compound.

Figure 1 shows XRD patterns for the Ru/MgO and Ru−Cs^+/MgO catalysts, which display comparatively intense diffraction reflections from the MgO phase along with weak, broadened reflections related to Ru metal. The sizes of Ru crystallites calculated from the width of Ru(001) reflections are given in Table 2. They are close to the $\langle d_{vs} \rangle$ values determined from TEM data on these samples. No peaks that may relate to any of the known cesium compounds with oxygen are observed in the XRD pattern of the Ru-Cs^+/MgO catalyst. In their turn, the TEM micrographs of this catalyst do not show any additional three-dimensional objects except for Ru particles and MgO globules. Thus, the XRD and TEM data allow us to suggest that the Cs promoter does not form a crystalline phase and is present as a surface.

Figure 2 shows high-resolution TEM micrographs from the Ru/MgO and Ru−Cs^+/MgO catalysts. With both samples, the HRTEM images of Ru particles exhibit periodic spacing closely matching the lattice spacing of Ru metal (a_{100} = 0.234 nm, a_{101} = 0.206 nm, etc.). In the micrographs of the Ru−Cs^+/MgO

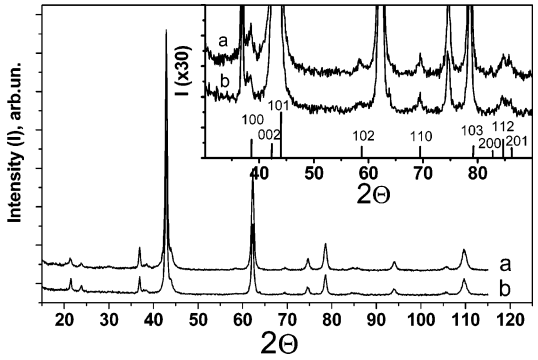

Figure 1. XRD patterns of (a) Ru/MgO and (b) Ru−Cs^+/MgO catalysts. The inset shows the region $30° \leq 2\theta \leq 90°$ of the XRD patterns after multiplication of the ordinate by 30 times. The marks in the inset indicate the exact positions and relative intensities of the diffraction reflections from the standard XRD pattern of metallic Ru (JCPDS no. 06−0663).

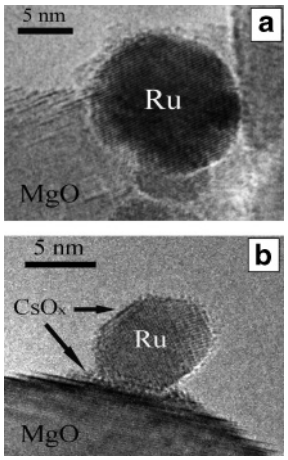

Figure 2. HRTEM micrographs of (a) Ru/MgO and (b) Ru−Cs^+/MgO catalysts. The arrows indicate the cesium-containing layer of disordered structure covering the surface of Ru particles and the areas of the support surface in the closest proximity to the Ru particles.

catalyst, the surface of the Ru crystallites is seen to be covered with a thin (subnanometer) layer of disordered structure. The HRTEM images of these overlayers exhibit contrast dots, indicating that the relatively heavy atoms (such as Cs atoms) are present in the covering layer. A similar layer also covers the areas of the MgO surface in closest proximity to the Ru particles, while this covering is not detected in the support surface regions farther than 5−10 nm from any Ru particle. The EDX spectrum of the surface region adjacent to a Ru particle in the Ru−Cs^+/MgO catalyst, which is shown in Figure 3, exhibits the peak at 4.3 keV assigned to the CsL signal along with the pattern of RuL peaks. Thus, the HRTEM/EDX data strongly suggest the presence of cesium in the overlayers on Ru crystal surface, as well as on the support regions adjacent to the Ru particles.

From Table 2, it is seen that the Ru dispersions calculated using the TEM and CO chemisorption data are in reasonable agreement for the Ru/MgO catalyst. The promotion does not have a significant impact on the dispersion as determined by TEM. On the contrary, Ru dispersion calculated from CO chemisorption data is reduced by about a factor of 2 (down to 6.2%) after adding the Cs promoter to the Ru/MgO catalyst. As is well-known,[24] the dispersion values obtained by TEM represent the entire surface area of metal particles, whereas the dispersion calculated from the chemisorption data only reflects the surface area exposed to the gas phase. On this basis, the

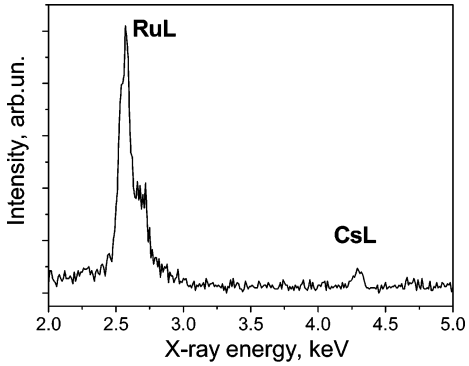

Figure 3. EDX spectrum obtained from the surface region around the Ru particle shown in Figure 2b.

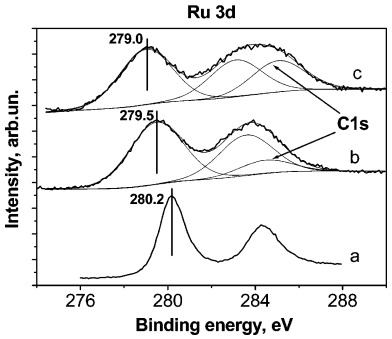

Figure 4. Ru 3d core level spectra of (a) polycrystalline Ru foil, (b) Ru/MgO, and (c) Ru−Cs^+/MgO catalysts. The arrows indicate the C 1s peaks derived from CH_x impurities originally present on the sample surface or slowly accumulated in the spectrometer.

difference between the dispersion calculated from the CO chemisorption and TEM data for the Ru−Cs^+/MgO catalysts can be ascribed to coverage of the Ru particles by the promoter layer.

Ru 3d Core Level Spectra. Figure 4 shows the Ru 3d core level spectra measured from the Ru/MgO and Ru−Cs^+/MgO samples. The Ru 3d spectrum from the Ru(poly) sample taken under identical conditions is also shown for comparison. The spectra consist of the Ru $3d_{5/2}$ and Ru $3d_{3/2}$ peaks appearing as a result of a spin-orbital splitting. The Ru $3d_{3/2}$ peak is overlapped with the C 1s peak at ∼285 eV derived from carbonaceous impurities (CH_x) originally present on the catalyst surface or slowly accumulated in the spectrometer. Consequently, only the values of E_b(Ru $3d_{5/2}$) are used in the following discussion. For the Ru/MgO and Ru−Cs^+/MgO samples, the E_b(Ru $3d_{5/2}$) values are 279.5 and 279.0 eV, respectively; these are by 0.7 and 1.2 eV lower than the value of E_b(Ru $3d_{5/2}$) observed for the bulk Ru metal (280.2 eV). The negative shift of the Ru 3d core level spectrum with respect to that of bulk Ru metal has been found for MgO-based ruthenium catalysts earlier[6,11] and accounted for by the transfer of electron density from the basic support to supported Ru metal particles.

Separation of Contributions of Initial and Final State Effects in the Ru $3d_{5/2}$ Binding Energy Variation. Meanwhile, the negative shift of the core level spectra from supported metal particles compared to the bulk metal may also be caused by the differential charging effect which appears for heterogeneous samples consisting of the phases with different conductivities when the less conductive phase is used as internal reference.[25,26] The internal reference method is effectively used for the homogeneously dielectric samples,[22] when charging, i.e., the surface positive charge accumulated as a result of photoelectron emission, equally affects the position of XPS peaks from all

elements contained in the sample. Then, it can be corrected by the shift of all XPS lines on the value which is the difference between the measured and tabulated E_b values of the reference peak. In the case of the heterogeneous systems like our catalysts, where metal particles are supported on a dielectric matrix, supported metallic nanocrystallites due to their internal conductivity can provide easier compensation of the positive charge induced by photoelectron emission than the dielectric support. As a result, the differential charging appears, i.e., the charging potential ϕ at the surface of a more conducting phase (e.g., supported Ru particles) is reduced in comparison with that of a less conducting phase (MgO support).[26] Consequently, if the XPS peak of dielectric support (e.g., the Mg 2s peak from MgO surface) is taken as an internal reference for correction of the E_b values for all XPS signals, an apparent negative shift of the peaks from supported metal particles on the value of $\Delta\phi = \phi$-(support) $- \phi$(metal) with respect to the peaks from bulk metal will appear.[25,26]

The differential charging value, $\Delta\phi$, can be estimated from the shift of the valence band spectrum of supported metal particles relative to that of bulk metal.[27,28] It is known that the Fermi levels of the bulk metal and the spectrometer are always in equilibrium. The Fermi level of the support is adjusted to that of the spectrometer by correction of the total charging with internal reference method. Thus, measuring the shift of the valence band spectrum obtained from the supported metal particles with respect to that from the bulk metal gives the difference between the Fermi levels of the dielectric support and the supported metal particles possessing the internal conductivity (i.e., the $\Delta\phi$ value). This approach leads to a reliable result only if any changes of the valence band spectrum caused by the small sizes of supported metal crystallites are not observed. The latter condition is implemented if the mean diameter of these particles is higher than 2 nm;[29] that is the case for our catalysts (see Table 2).

Another final state effect which can contribute to variation of the E_b value is the well-known relaxation effect representing a change in the relaxation energy due to reorganization of electrons of the solid that provides the screening of the photoelectron holes remaining after electron emission.[29−31] The variation of the relaxation energy, ΔE_R, can be estimated from the following relation

$$\Delta E_R = 0.5 \times \Delta\alpha \quad (1)$$

where $\Delta\alpha$ is the change in the value of the modified Auger parameter, α, that represents the sum of a core level binding energy and a kinetic energy of the most prominent Auger peak and can be experimentally determined.[30] In the case of ruthenium

$$\alpha = E_b(\text{Ru } 3d_{5/2}) + E_{kin}(\text{Ru MNN}) \quad (2)$$

where E_{kin}(Ru MNN) is the kinetic energy of the Auger Ru MNN transition.

With the relaxation effect taken into account, the binding energy shift measured for supported metal crystallites with respect to a certain standard, typically, to the bulk metal, ΔE_b, can be written as[30,31]

$$\Delta E_b = \Delta E - \Delta E_R \quad (3)$$

where ΔE is the "true" chemical shift, which reflects the difference between energies of the initial states of the studied metal in the supported metal particles and in the bulk metal.

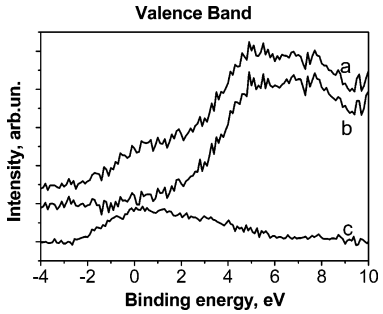

Figure 5. Valence band spectra of (a) Ru−Cs^+/MgO catalyst and (b) Cs^+/MgO sample. The difference between the curves a and b is plotted below (curve c).

The choice of the sign in eq 3 is due to the fact that the relaxation effect results from rearrangement of $N - 1$ electrons which tend to screen core holes remaining after electron emission. This screening will always act effectively to increase the kinetic energy of the photoelectrons, i.e., to decrease the apparent binding energy.[29,32] From eq 3, the variation of orbital energies (initial state effect) for Ru atoms in the supported Ru particles (Ru_{sup}) with respect to the bulk metal (Ru_{bulk}) is given by

$$\Delta E = [E_b(Ru_{sup}) - E_b(Ru_{bulk})] + [E_R(Ru_{sup}) - E_R(Ru_{bulk})] \quad (4)$$

Parameter α and, hence, E_R values are not dependent (in the first approximation) on the charging, because increasing the core level binding energy with an increase in the charging potential is compensated for by a decrease in the Auger kinetic energy by the same value. Consequently, the α value measured for a sample does not change as a result of correction for the charging effect, even if the differential charging occurs. Contrary to this, the value of $E_b(Ru_{sup})$ in eq 4 should be corrected for the $\Delta\phi$ value

$$\Delta E = [E_b(Ru_{sup}) + \Delta\phi - E_b(Ru_{bulk})] + [E_R(Ru_{sup}) - E_R(Ru_{bulk})] = \Delta E_b + \Delta\phi + \Delta E_R \quad (5)$$

In order to determine the ΔE_R and $\Delta\phi$ values for supported ruthenium in the Ru/MgO and Ru−Cs^+/MgO catalysts compared to the bulk metal, the corresponding Ru MNN Auger and valence band spectra should be measured.

Valence Band Spectra. The valence band spectra measured for the Ru/MgO and Ru−Cs^+/MgO catalysts contain the contributions of the support and promoter (if the latter is present in the catalyst) in addition to the signals from the valence Ru 4d/5s orbitals. In order to extract the contribution of supported ruthenium, the valence band spectra from the MgO and Cs^+/MgO samples were also measured and subtracted from the spectra of the Ru/MgO and Ru−Cs^+/MgO catalysts, respectively. Prior to the subtraction procedure, all the spectra were normalized to the XPS intensities in the E_b region of 5−8 eV where the contribution from ruthenium is minimal. As an example, the experimental valence band spectra of Ru−Cs^+/MgO and Cs^+/MgO samples as well as the corresponding difference spectrum are demonstrated in Figure 5.

Figure 6 compares the difference valence band spectra of the supported ruthenium in the Ru/MgO and Ru−Cs^+/MgO catalysts with the spectrum measured for the Ru(poly) sample. Aligning the valence band spectrum of the bulk metallic ruthenium up to the perfect coincidence with the spectrum of the supported ruthenium makes it possible to establish that the Fermi levels of the supported Ru in the Ru/MgO and Ru−Cs^+/

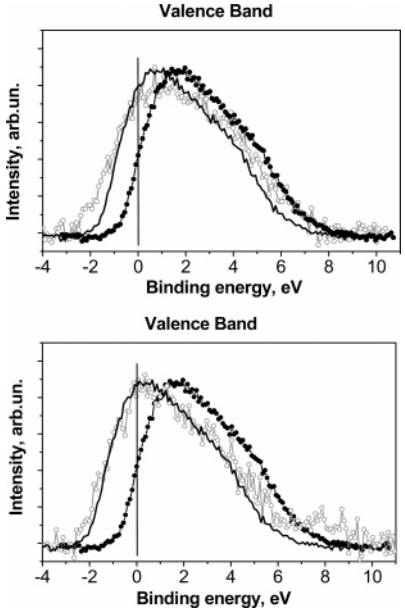

Figure 6. Comparison of the valence band spectra position for supported and bulk ruthenium metal. The curves with open circles are the difference valence band spectra of supported ruthenium in the Ru/MgO (top panel) and Ru−Cs^+/MgO (bottom panel) catalysts. The dashed and solid lines show the observed valence band spectrum of polycrystalline Ru foil and the same spectrum shifted by 1.0 (top panel) or 1.3 (bottom panel) eV, respectively.

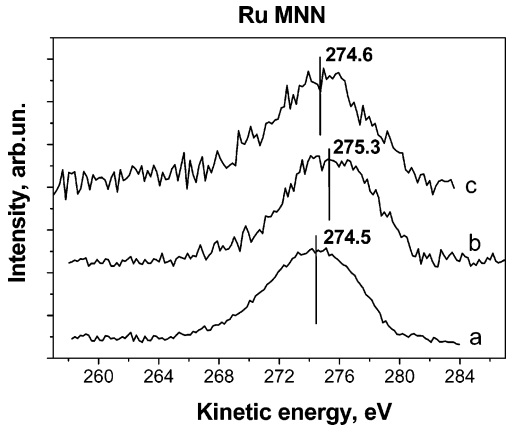

Figure 7. Auger Ru MNN spectra of (a) polycrystalline Ru foil and (b) Ru/MgO sample. (c) Difference spectrum of supported ruthenium obtained by subtraction of the Cs 3s core level spectrum of Cs^+/MgO sample from the Auger Ru MNN spectrum of Ru−Cs^+/MgO catalyst.

MgO catalysts are shifted by 1.0 and 1.3 eV, respectively, toward lower E_b with respect to the Fermi level of bulk Ru metal. From TEM and XRD data (see Table 2), the mean diameter of supported Ru crystallites is as large as ca. 5 nm in the studied catalysts; therefore, the shift of the valence band spectrum can be attributed exclusively to the differential charging effect. The value of this shift represents the $\Delta\phi$ value.[32] Correspondingly, the Ru 3d core level spectra measured for the Ru/MgO and Ru−Cs^+/MgO catalysts (see Figure 4) should be shifted to higher E_b by the $\Delta\phi$ values, which are equal to 1.0 and 1.3 eV, respectively.

Auger Ru MNN Spectra. Figure 7 (curves a and b) shows the Ru MNN Auger spectra measured for the Ru(poly) and Ru/MgO samples. Since the Ru MNN spectrum of the promoted catalyst is overlapped with XP 3s line from cesium, the Cs 3s core level spectrum of the reference Cs^+/MgO sample was measured and subtracted from the overall (Ru MNN + Cs 3s) spectrum of the Ru−Cs^+/MgO catalyst. Before subtraction, the spectra were normalized to the XPS intensities in the kinetic energy range of 260−265 eV where the contribution from ruthenium was minimal. The difference spectrum thus obtained is present in Figure 7 (curve c).

TABLE 3: Experimental Ru $3d_{5/2}$ Binding and Ru MNN Auger Kinetic Energies for the Ru/MgO, Ru−Cs^+/MgO, and Polycrystalline Ruthenium Foil (Ru(poly)) Samples, Values of Final State Effects Derived from These Data, and Energy Differences between the Initial States of Supported and Bulk Ruthenium Metal Calculated by Eq 6[a]

sample	E_b (Ru$3d_{5/2}$)	ΔE_b	$\Delta\phi$	E_{kin} (RuMNN)	α	ΔE_R	ΔE
Ru(poly)	280.2	0	0	274.5	554.7	0	0
Ru/MgO	279.5	−0.7	1.0	275.3	554.8	+0.05	+0.35
Ru-Cs^+/MgO	279.0	−1.2	1.3	274.6	553.6	−0.55	−0.45

[a] E_b(Ru $3d_{5/2}$) and E_{kin}(Ru MNN) are the experimental Ru $3d_{5/2}$ binding energy and Ru MNN kinetic energy, respectively; ΔE_b is the difference between the Ru $3d_{5/2}$ binding energies measured for supported and bulk Ru metal; $\Delta\phi$ is the differential charging value (the difference between the charging potentials at the MgO surface and at the surface of supported Ru particles) determined from the shift of the valence band spectrum of supported Ru with respect to that of bulk Ru metal (see Figure 6); α is the modified Auger parameter defined as $\alpha = E_b$(Ru $3d_{5/2}$) + E_{kin}(Ru MNN); ΔE_R is the variation of relaxation energy defined as $\Delta E_R = 0.5\Delta\alpha$, where $\Delta\alpha$ is the Auger parameter shift between supported and bulk Ru metal; ΔE is the energy difference between the initial states of supported and bulk Ru metal calculated as $\Delta E = \Delta E_b + \Delta\phi + \Delta E_R$. All values in this table are given in eV.

The α values calculated by eq 2 from the experimental binding Ru $3d_{5/2}$ and kinetic Auger Ru MNN energies coincide for the Ru(poly) and Ru/MgO samples with an accuracy to 0.1 eV (554.7 and 554.8 eV, respectively). The value of $\Delta\alpha = 0.1$ eV, which is equal to the XPS detection limit, corresponds to a very small value of the ΔE_R ($\Delta E_R = 0.05$ eV) and indicates that the relaxation gives essentially no contribution to the variation in the Ru 3d spectrum of the Ru/MgO sample. For the Ru−Cs^+/MgO catalyst, the value of α is equal to 553.6 eV and less by 1.1 eV than the corresponding value for bulk Ru metal. Correspondingly, the change in the relaxation energy for the Ru−Cs^+/MgO catalyst as compared with metallic Ru is quite considerable and has a negative value ($\Delta E_R = -0.55$ eV).

Table 3 summarizes all the parameters (E_b(Ru $3d_{5/2}$), ΔE_b, E_{kin}(Ru MNN), α, and ΔE_R) found for the Ru(poly), Ru/MgO, and Ru−Cs^+/MgO samples by means of Ru 3d core level, valence band, and Ru MNN Auger spectra, as well as the energy differences between the initial states of supported and bulk Ru metal calculated by eq 5. The Ru $3d_{5/2}$ orbital energy for the Ru/MgO sample (280.55 eV) is 0.35 eV greater than the corresponding value for the Ru(poly) sample (280.2 eV). Hence, the negative shift of the Ru 3d peak by 0.7 eV observed for this catalyst is caused by the differential charging and not related to the presence of a negative charge on the surface of Ru crystallites. The corrected value of E_b(Ru $3d_{5/2}$) for the Ru−Cs^+/MgO catalyst is 279.75 eV, i.e., it remains lower than that of the bulk Ru metal. Thus, a decrease in the energy caused by the differential charging and is not related to the presence of a negative charge on the surface of Ru crystallites. The corrected value of E_b(Ru $3d_{5/2}$) for the Ru−Cs^+/MgO catalyst is 279.75 eV, i.e., it remains lower than that of the bulk Ru metal. Thus, a decrease in the energy of the initial state of Ru atoms ($\Delta E = -0.45$ eV) is only observed when the supported Ru catalyst is promoted with cesium.

After the correction for the differential charging (Table 3), the E_b(Ru $3d_{5/2}$) value is even higher for the Ru/MgO sample than for bulk Ru metal. The corrected value of E_b(Ru $3d_{5/2}$) = 280.55 eV determined for the Ru/MgO catalyst is similar to

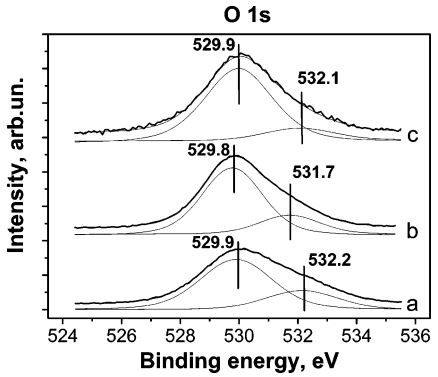

Figure 8. O 1s core level spectra of (a) MgO support, (b) Ru/MgO, and (c) Ru−Cs^+/MgO catalysts.

that found earlier[17] for Ru nanoparticles supported on Al_2O_3 or SiO_2, although the surface of these supports, unlike the MgO surface, does not contain the strong basic sites.

O 1s Core Level Spectra. Figure 8 shows the O 1s core level spectra of Ru/MgO and Ru−Cs^+/MgO catalysts in comparison with the spectrum of MgO. Each spectrum contains an asymmetric peak which can be decomposed into two features related to different surface states of oxygen. The main feature at ca. 530 eV is assigned to O^{2-} ions of MgO lattice. The maxima of this feature coincide for all the samples within the accuracy of E_b determination. The less intense feature at ca. 532 eV may be assigned to OH groups on the MgO surface.[33] In the spectrum of Ru/MgO catalyst, this feature is shifted by 0.5 eV to lower E_b with respect to the same peak in the spectrum of MgO. This shift indicates an increase in the negative charge on oxygen atoms of the surface OH groups in the Ru/MgO sample as compared with MgO containing no supported ruthenium. In the spectrum of Ru−Cs^+/MgO catalyst, the less intense feature practically matches that in the spectrum of the support (532.2 and 532.1 eV, respectively).

Examination of the Chemical State of Cs Promoter. The Cs $3d_{5/2}$ core level spectra of Ru−Cs^+/MgO and Cs^+/MgO samples were recorded in order to identify the chemical state of Cs promoter in the promoted catalyst. Initially, the spectrum was registered with a sample exposed to air for short period of time ($\Delta t \leq 5$ min) that was required for loading of the samples inside the spectrometer. The samples of this kind are hereinafter referred to as "oxidized" samples, $(Ru-Cs^+/MgO)_{ox}$ and $(Cs^+/MgO)_{ox}$. Then, the Cs $3d_{5/2}$ spectra were recorded with the same samples treated with H_2 at 350 °C and 101 kPa for 1 h in the preparation chamber of spectrometer ("reduced" samples, $(Ru-Cs^+/MgO)_{red}$ and $(Cs^+/MgO)_{red}$). The corresponding spectra are shown in Figure 9.

The Cs $3d_{5/2}$ spectrum of the $(Ru-Cs^+/MgO)_{ox}$ sample (Figure 9, curve a) exhibits a peak at 724.7 eV that is intermediate between the E_b(Cs $3d_{5/2}$) values found for thin surface layers of cesium oxide and peroxide on various substrates (725.2 and 724.5 eV for Cs_2O and Cs_2O_2, respectively).[34,37] The treatment of the $(Ru-Cs^+/MgO)_{ox}$ sample with H_2 leads to the shift of 724.7 eV peak to 725.5 eV (Figure 9, curve b). It is known[34−37] that an inverse correlation between the binding energy and the oxidation state of the metal (when the value of E_b for the metal is higher than the E_b values for the same metal in its oxides) is observed for cesium as well as for some other metals (e.g., silver, cadmium, or barium). Hence, one can suppose that the observed positive shift of the Cs $3d_{5/2}$ peak results from reduction of Cs^+ ions by H_2. At the same time, the value of E_b(Cs $3d_{5/2}$) = 725.5 eV found for the $(Ru-Cs^+/MgO)_{red}$ sample is considerably lower than the value given

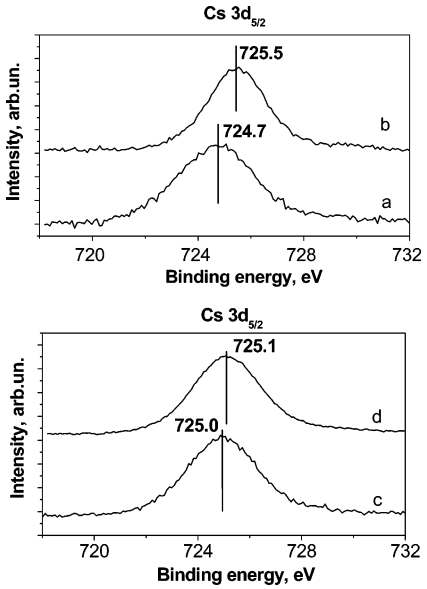

Figure 9. Cs $3d_{5/2}$ core level spectra of (top panel) Ru−Cs^+/MgO and (bottom panel) Cs^+/MgO samples (a,c) exposed to air for short time and (b,d) treated with H_2 at 350 °C and 101 kPa in the preparation chamber of spectrometer.

TABLE 4: Binding Energies and Cs/O Atomic Ratios Obtained by XPS for the Model Samples Prepared by Deposition of a Cs + O Coadsorbate Layer on the Surface of Polycrystalline Ru Foil

	binding energy (eV)			
deposition technique	Cs $3d_{5/2}$	O 1s	Cs/O atomic ratio[a]	assignment
in flowing O_2 (0.01 P)	725.0	530.5	0.83	Cs_2O_2
in vacuum ($<5 \times 10^{-7}$ Pa)	725.8	531.5	1.90	$Cs_{2+x}O$

[a] Calculated from the integral intensities of the Cs $3d_{5/2}$ and O 1s peaks using the corresponding atomic sensitivity factors taken from ref 22.

in ref 38 for Cs metal (726.2 eV). That is why we can exclude the presence of cesium metal in the Ru−Cs^+/MgO catalyst after the high-temperature treatment with H_2 but assume that cesium peroxide is reduced by H_2 to Cs_2O and then to cesium suboxide $Cs_{2+x}O$. For the $(Cs^+/MgO)_{ox}$ sample, the Cs $3d_{5/2}$ binding energy is very close to that of the $(Ru-Cs^+/MgO)_{ox}$ sample and not changed noticeably after the treatment of the $(Cs^+/MgO)_{ox}$ sample with H_2 in the spectrometer chamber (Figure 9, bottom panel).

Finally, we examined the chemical state of cesium in the model samples prepared by deposition of metallic Cs vapor on the surface of polycrystalline Ru foil both in vacuum and in flowing O_2. While O 1s peaks derived from cesium oxygen species can be masked by the peaks from OH groups or O^{2-} ions of MgO, the substitution of the model Ru(poly) support for magnesia makes it possible to use the O 1s core level spectra along with the Cs $3d_{5/2}$ spectra for identification of these species. The Cs $3d_{5/2}$ and O1s binding energies as well as the $(Cs/O)_{sur}$ atomic ratios obtained by XPS for the model samples are summarized in Table 4. When cesium is evaporated in flowing O_2 at 0.01 Pa, the value of E_b(Cs $3d_{5/2}$) = 725.0 eV is very close to that found for the $(Ru-Cs^+/MgO)_{ox}$ and $(Cs^+/MgO)_{ox}$ samples. The O 1s spectrum of the model sample shows an intense peak at 530.5 eV along with a less intense feature at 533.5 eV, which can be assigned to surface cesium peroxide Cs_2O_2 and cesium superoxide Cs_2O_4, respectively.[37,39] For the sample prepared via Cs evaporation in flowing O_2, the (Cs/

$O)_{sur}$ atomic ratio is equal to 0.83, which is close to the 1:1 stoichiometry of Cs_2O_2 (some deviation of the experimental $(Cs/O)_{sur}$ value from the expected value of $(Cs/O)_{sur} = 1.0$ may be accounted for by the presence of Cs_2O_4). When cesium is evaporated in vacuum ($P < 5 \times 10^{-7}$ Pa), the O 1s peak is observed at 531.5 eV and may be assigned to cesium suboxide, $Cs_{2+x}O$[34] that is formed due to oxidation of cesium metal with O_2 traces in the spectrometer. The fact that the O 1s peak at 531.5 eV appears along with a Cs $3d_{5/2}$ peak at 725.8 eV confirms the suggested assignment of the Cs $3d_{5/2}$ peak at around 725.5 eV to $Cs_{2+x}O$. However, the $(Cs/O)_{sur}$ ratio was found to be slightly less than 2.0 for the sample prepared by evaporation of cesium onto Ru(poly) in vacuum (see Table 4). This discrepancy may be accounted for by partial oxidation of the surface of the $Cs_{2+x}O$ layer by traces of O_2 in the spectrometer.

The Ru 3d core level spectra were also measured for the model samples prepared by deposition of metallic Cs vapor on the Ru(poly) surface. Regardless of the evaporation conditions (in vacuum or in an O_2 flow), the E_b(Ru $3d_{5/2}$) value was found the same as for the Ru(poly) sample containing no cesium (280.2 eV).

Discussion

The activity of Ru−Cs^+/MgO catalyst toward ammonia synthesis at 250−400 °C and 101 kPa of 1:3 N_2/H_2 gas mixture is higher by more than an order of magnitude of the activity of nonpromoted Ru/MgO catalyst (Table 1). This result agrees with the literature data,[7,11] indicating that the catalyst samples prepared in this work can be used as objects for studying the support and promoter effects which are discussed in the literature (see Introduction).

XRD and TEM data presented in Figure 1 and Table 2 show that the Cs promotion does not significantly alter the mean Ru particle size or the mode of particle size distribution. Consequently, the increase in activity cannot be explained solely by the difference in Ru dispersion between the promoted and nonpromoted catalysts. On the other hand, XPS indicates the difference between the Ru $3d_{5/2}$ binding energies for surface Ru atoms in the Ru/MgO and Ru−Cs^+/MgO catalysts (Figure 4); in the both cases, the Ru $3d_{5/2}$ peak is shifted to lower E_b compared to that for the bulk metallic Ru. The use of valence band and Auger Ru MNN spectra (Figures 6 and 7) for determination of the final state contributions reveals that the negative shift of the Ru 3d core level spectrum observed for the Ru/MgO catalyst does not reflect a change in the initial state of supported ruthenium as compared with the metallic one, but is caused mainly by the alteration in the differential charging of supported Ru particles compared with the support surface. After the correction for the differential charging (Table 3), the E_b(Ru $3d_{5/2}$) value is even higher for the Ru/MgO sample than for bulk Ru metal. The corrected value of E_b(Ru $3d_{5/2}$) = 280.55 eV determined for the Ru/MgO catalyst is similar to that found earlier[17] for Ru nanoparticles supported on Al_2O_3 or SiO_2, although the surface of these supports, unlike the MgO surface, does not contain the strong basic sites.

The positive shift of Ru $3d_{5/2}$ peak is accompanied by the negative shift of the O 1s peak at ca. 532 eV, which can be assigned to the OH groups on the support surface. This peak is shifted by 0.5 eV to lower E_b values relative to that in the spectrum of MgO containing no supported ruthenium (Figure 8). It allows the suggestion that there is electron transfer from the supported Ru particles to OH groups on the MgO surface. At the same time, we did not observe any shift of another O 1s peak at around 530 eV assigned to the lattice oxygen in MgO that would indicate the electron density transfer from the lattice O^{2-} ions to supported metal crystallites. The absence of the shift does not suggest unambiguously that the electron donation from the lattice O^{2-} ions does not occur, since it is hardly to exclude that this interaction remains unnoticed due to its weakness or the considerably higher surface content of O^{2-} ions as compared with the atomic Ru content. Nevertheless, the resulting electronic effect of the MgO surface on supported Ru particles is the electron-withdrawing one but not electron-donating, as reported before.[6,7,13] Perhaps, this is not a general conclusion but only valid for the supported Ru catalysts prepared from Ru chlorides, because the presence of Cl^- impurity usually increases the acidity of surface groups on the support.[40]

For the Ru−Cs^+/MgO catalyst, the experimental E_b(Ru $3d_{5/2}$) value is contributed by the differential charging ($\Delta\phi = 1.3$ eV) along with the relaxation effect ($\Delta E_R = -0.55$ eV). After the correction for these final state contributions, the negative shift of the Ru $3d_{5/2}$ peak with respect to that of the bulk Ru metal ($\Delta E = -0.45$ eV) is still observed. The O 1s core level spectrum of the Ru−Cs^+/MgO catalyst matches that of MgO, indicating the absence of any significant interaction between Ru atoms and surface sites (O^{2-} ions, OH groups) of the support. The results obtained allow us to suppose the change in the initial state of surface Ru atoms in the Ru−Cs^+/MgO catalyst as compared with metallic one, and this is mainly due to the interaction of the Ru particles with the Cs promoter but not with the support.

HRTEM/EDX analysis shows that the Cs promoter is present in the Ru−Cs^+/MgO catalyst as a thin layer of disordered structure on the surface of the Ru crystallites (Figures 2 and 3). Table 2 demonstrates that the Ru dispersion of the promoted catalyst obtained from TEM is larger than that obtained by CO chemisorption. This effect can be ascribed to covering of the Ru particles by the promoter layer. At the same time, the dispersion obtained by CO chemisorption is far enough from zero, indicating that the layer of cesium oxide over the surface of Ru particles is not continuous and some surface Ru atoms are exposed to gaseous reagents. The promoter layer also covers the areas of the MgO surface adjoining the Ru particles, but it is not observed at a distance from any Ru particle. This fact strongly suggests that the promoter is preferably located on the surface of Ru crystallites and bonded to them strongly enough. As a result, the cesium-containing layer cannot migrate from the ruthenium surface to the support but within small areas of the support surface being in close proximity to the Ru crystallites. As reported before,[37] the cesium-oxygen layer can be fixed on the silver metal surface through formation of Ag−Cs bonds. We can suggest by analogy that upon introduction of the Cs promoter into a supported Ru catalyst the chemical bonds between cesium atoms and the transition metal (Ru) atoms are also formed.

Since no crystalline phases containing cesium are present in the Ru−Cs^+/MgO catalyst, the information about the chemical state of the promoter can be obtained only from the Cs $3d_{5/2}$ core level spectra. Comparing the Cs $3d_{5/2}$ binding energies measured both before and after treatment of the promoted catalyst with H_2 in photoelectron spectrometer (Figure 9) with the literature data[34−38] on the known cesium compounds and taking into account the inverse correlation between E_b(Cs $3d_{5/2}$) and the oxidation state of Cs, we assume that the promoter layer treated with H_2 mainly comprises cesium suboxide, $Cs_{2+x}O$, which represents cesium oxide with a faulted crystal structure containing a large number of oxygen vacancies. The bulk cesium suboxides such as Cs_7O and $Cs_{11}O_3$ have been described in the

literature.[35] The formation of nonstoichiometric cesium suboxides during the controlled oxidation of metallic cesium films evaporated onto Ag substrate was observed using ultraviolet photoelectron spectroscopy[41] and XPS.[34,37] In ref 37, the formation of surface cesium suboxide upon reduction of the $Ag-Cs^+/Al_2O_3$ catalyst was supposed as a result of the comparison of XPS and temperature-programmed desorption data obtained for the supported catalyst and for Ag(111) or Ag(110) single crystals covered by the cesium oxide film. In the course of preparation of $Ru-Cs^+/MgO$ catalyst for ammonia synthesis, cesium suboxide may arise at the final stage, when the Ru/MgO sample impregnated with cesium carbonate is treated in a H_2 flow at the temperature as high as 450 °C for a long period of time. During this procedure, Cs_2CO_3 is probably decomposed to the Cs_2O overlayer with oxygen vacancies appeared therein. The contact of the H_2-treated catalyst with atmospheric dioxygen (for example, during the sample loading to the spectrometer chamber) results in a fast conversion of both $Cs_{2+x}O$ and Cs_2O into Cs_2O_2, that explains lower E_b (Cs $3d_{5/2}$) binding energy observed with the $(Ru-Cs^+/MgO)_{ox}$ sample as compared with the $(Ru-Cs^+/MgO)_{red}$ sample. The oxidized surface layer containing Cs_2O_2 alone or in the mixture with Cs_2O can be re-reduced with H_2 to obtain $Cs_{2+x}O$ even under static conditions.

The Cs $3d_{5/2}$ core level spectrum of the Cs^+/MgO sample measured after its loading in the spectrometer (i.e., immediately after contact with atmospheric O_2) also exhibits the peak at 725.0 eV indicating the presence of Cs_2O_2 (probably in the mixture with Cs_2O). However, in this case the peak is not shifted toward higher E_b upon the treatment of the sample with H_2 in the spectrometer chamber (see Figure 9). As shown experimentally,[42] unsupported Cs_2O_2 is not reduced with H_2 into CsOH at 400−500 °C but in the mixture with Ru metal. It is reasonable to suppose that the reduction of surface Cs_2O_2 into Cs_2O and formation of oxygen vacancies in Cs_2O also occur exclusively in the presence of Ru metal. As suggested before,[21] the surface Ru atoms in supported Ru catalysts may be the sites for H_2 dissociation with the formation of atomic hydrogen that is a stronger reducing agent than H_2. Thus, the reduction of Cs_2O_2 and Cs_2O into $Cs_{2+x}O$ may proceed at the interface between the supported Ru particles and cesium-containing layer which covers the surface of Ru crystallites in the promoted catalyst.

There are at least two different ways to explain why the coverage of the supported ruthenium crystallites with the cesium-containing layer gives rise to a decrease in the Ru 3d binding energy. The conventional explanation is that the Cs promoter donates electrons to ruthenium to cause the negative charging of the metal particles ("charge transfer" mechanism).[6,13,14] Another phenomenon that may be responsible for decreasing of the Ru 3d binding energy is a reduction of the work function of ruthenium due to the formation of an electric double layer with the participation of Cs^+ cations and surface Ru atoms at the interface between supported Ru particles and their cesium−oxygen coverings. Lowering the work function for a transition metal as a result of its coating with an alkali metal−oxygen film has been reported in many papers[34,43] and is used in various practical photoemission devices such as cesium−silver S-1 photocathodes.[34]

If a conducting sample containing a metal is in electrochemical equilibrium with a spectrometer, the apparent binding energy of an electron in a metal that is normally given with respect to the Fermi level of a spectrometer does not depend on variations in the work function of the sample

$$E_{kin} = h\nu - E_b - \varphi_{sp} \quad (6)$$

where $h\nu$ is the irradiation energy, E_{kin} and E_b are the kinetic and binding energies of the emitted electron, respectively, and φ_{sp} is the work function of the spectrometer. However, if the metal particles are localized on the surface of a dielectric support (for example, on the MgO surface), when the Fermi levels of the metal and a spectrometer are not in equilibrium, variations in the work function of the sample must give rise to an apparent binding energy shift for the supported metal with respect to that for the bulk metal. In particular, a decrease in the work function of the supported metal (for example, under influence of an alkali promoter) must shift the apparent binding energy downward.

In our opinion, a "charge transfer" mechanism can be suggested with a great degree of confidence only if the promoting layer contains metallic cesium. However, the XPS measurements do not reveal the presence of metallic cesium in the $Ru-Cs^+/MgO$ catalyst even after high-temperature treatment with H_2. Cesium suboxides $Cs_{2+x}O$ that contain numerous oxygen vacancies also may serve as electron donors, in contrast to Cs_2O_2 or Cs_2O. If electrons are indeed transferred from the $Cs_{2+x}O$ layer to Ru atoms, one can expect changes in the chemical state of Ru atoms after the promoted catalyst has been treated with H_2 to cause the conversion of Cs_2O_2 to $Cs_{2+x}O$. In reality, the treatment of the $Ru-Cs^+/MgO$ catalyst with H_2 did not alter the Ru $3d_{5/2}$ binding energy. This fact makes it doubtful that the downward shift of the Ru 3d peaks observed for the promoted catalyst as compared with the nonpromoted sample is caused by the negative charging of the supported Ru crystallites.

As to the alternative explanation, the results of our recent studies[44,45] on $Ru-Cs^+/C$ catalysts exhibiting fairly high catalytic activity in ammonia synthesis provide an additional argument in the favor of the proposal that the downward shift of the Ru 3d spectrum is caused by a decrease in the work function of the supported ruthenium under the influence of a cesium−oxygen overlayer. For the $Ru-Cs^+/C$ catalyst, surface coverings containing cesium and oxygen were detected[45] on Ru crystallites similar to that observed for the $Ru-Cs^+/MgO$ catalyst. Nevertheless, the negative shift in the Ru $3d_{5/2}$ binding energy was not observed for metallic ruthenium when it was supported onto a carbon material of high conductivity.

Even though the experimental data are not sufficient yet to conclude unambiguously the reasons for the change in the initial state of supported ruthenium under the influence of cesium promoter, it is important that both of the suggested effects (negative charge transfer or lowering the work function of Ru) should result in the accumulation of the electron density on the surface Ru atoms. This will facilitate the transfer of d electrons from Ru atoms to the antibonding molecular orbitals of adsorbed N_2 molecules and therefore promote N_2 dissociation that is the rate-determining step of ammonia synthesis. Thus, lowering the work function of ruthenium metal by covering it with a cesium−oxygen layer should affect the catalytic activity of Ru for ammonia synthesis the same way as the electron donation from an alkali metal (or an alkali metal compound) to Ru atoms.

Summary

The negative shift of the experimental Ru 3d core level spectrum which is observed for the supported Ru/MgO catalysts with respect to that of the bulk Ru metal has long been accounted for by the transfer of electron density from basic sites of the support. Contrary to this opinion, we found that the shift is caused by the differential charging of the supported ruthenium

compared with the support surface. This phenomenon originates from the higher internal conductivity of the supported ruthenium than that of the dielectric support (MgO). The contribution of the differential charging in the total variation of binding energy is usually not taken into account when studying supported metal catalysts by XPS. The apparent Ru $3d_{5/2}$ binding energy, if corrected for this effect, proves to be 280.5 eV, i.e., by 0.3 eV higher than that of metallic ruthenium and very close to that previously communicated for Ru/Al_2O_3 or Ru/SiO_2. This fact indicates that the supported Ru particles in the Ru/MgO catalyst are positively charged, probably, due to the interaction with surface OH groups of magnesia. Thus, the difference in ammonia synthesis activity between the Ru catalysts supported on MgO and on the acidic supports (Al_2O_3, SiO_2) is caused not by the different electronic state of ruthenium on these oxides but by other reasons. Further studies are in progress in order to clarify these reasons.

Addition of a Cs promoter to the Ru/MgO catalyst does not have a significant impact on Ru dispersion. The promoter is present as a thin amorphous layer that partly covers the surface of Ru crystallites and adjacent surface areas. After the treatment with H_2 at 450 °C, the promoter layer is thought to consist mainly of cesium suboxide $Cs_{2+x}O$, which is a cesium oxide with a faulted crystal structure including numerous oxygen vacancies. In the presence of O_2, $Cs_{2+x}O$ is readily transformed into cesium peroxide Cs_2O_2 or into a $Cs_2O_2 + Cs_2O$ mixture.

For the $Ru-Cs^+/MgO$ catalyst, the Ru $3d_{5/2}$ binding energy, even though corrected for the differential charging and relaxation effects, remains negatively shifted. Hence, we can assert that a decrease in the binding energy observed for the supported ruthenium is a result of coverage of the Ru particles with a cesium oxygen layer. Although it is hardly possible to elucidate unambiguously the reasons for this negative shift (electron transfer from the Cs promoter to the supported Ru particles vs lowering the work function of supported ruthenium), the excess of electron density on the surface Ru atoms realized as a result of both phenomena must favor a decrease in the energy barrier of dissociative chemisorption of N_2, which is the most difficult step of ammonia synthesis. As a consequence, we can conclude that the close contact between Ru particles and the Cs promoter needs to be provided for the promoted ruthenium catalyst to reveal sufficiently high catalytic activity to ammonia synthesis.

Acknowledgment. The work was supported by the Russian Foundation for Basic Research (the project code 02-03-32681) and the Russian Academy of Sciences (integral project no. 10.4). One of the authors (Yu.V. L.) also acknowledges the K. Zamaraev International Charitable Scientific Foundation for the financial support. The authors thank Prof. A. S. Ivanova and Mrs. N. V. Karasyuk for the preparation of MgO, Prof. E. M. Moroz for XRD measurements, Prof. A. S. Lisitsyn and Dr. L. B. Okhlopkova for CO chemisorption measurements, Mrs. I. L. Kraevskaya for X-ray fluorescence analysis, and Dr. I. P. Prosvirin for experimental assistance.

References and Notes

(1) Schloegl, R. In *Handbook of Heterogeneous Catalysis*; Ertl, G.; Knozinger, H.; Weitkamp, J., Eds.; Wiley-VCH: Weinheim, Germany, 1997; Vol. 4, Chapter 2.1, p 1697.

(2) Czuppon, T. A.; Knez, S. A.; Schneider, R. V.; Worobets, G. *Chem. Eng.* **1993**, *100*, 19.

(3) Kowalczyk, Z.; Jodzis, S.; Rarog, W.; Zielinski, J.; Pielaszek, J. *Appl. Catal., A* **1998**, *173*, 153.

(4) Aika, K.; Niwa, Y. In *Studies in Surface Science and Catalysis*; Hattori, H., Otsuka, K., Eds.; Elsevier Science: Tokyo, 1999; Vol. 121, p 327.

(5) Bielawa, H.; Hinrichsen, O.; Birkner, A.; Muhler, M. *Angew. Chem., Int. Ed.* **2001**, *40*, 1061.

(6) Aika, K.; Ohya, A.; Ozaki, A.; Inoue, Y.; Yasumori, Y. *J. Catal.* **1985**, *92*, 305.

(7) Aika, K.; Takano, T.; Murata, S. *J. Catal.* **1992**, *136*, 126.

(8) Khaja, M. S.; Rama, R. K. S.; Rama, R. P. *Indian J. Chem., Ser. A* **1993**, *32*, 383.

(9) Yunusov, S. M.; Moroz, B. L.; Ivanova, A. S.; Likholobov, V. A.; Shur, V. B. *J. Mol. Catal. A: Chem.* **1998**, *132*, 263.

(10) Moggi, P.; Predieri, G.; Maione, A. *Catal. Lett.* **2002**, *79*, 7.

(11) Muhler, M.; Rosowski, F.; Hinrichsen, O.; Hornung, A.; Ertl, G. In *Studies in Surface Science and Catalysis*; Hightower, J. W., Delglass, W. N., Iglesia, E., Bell, A. T., Eds.; Elsevier Science: New York, 1996; Vol. 101, p 317.

(12) Yunusov, S. M.; Likholobov, V. A.; Shur, V. B. *Appl. Catal., A* **1997**, *158*, L35.

(13) Aika, K.; Tamaru, K. In *Ammonia: Catalysis and Manufacture*; Nielsen, A., Ed.; Springer: Berlin, 1995; p 104.

(14) Aika, K.; Kubota, J.; Kadowaki, Y.; Niwa, Y.; Izumi, Y. *Appl. Surf. Sci.* **1997**, *121/122*, 488.

(15) Hinrichsen, O.; Rosowski, F.; Hornung, A.; Muhler, M.; Ertl, G. *J. Catal.* **1997**, *165*, 33.

(16) Dahl, S.; Logadottir, A.; Jacobsen, C. J. H.; Norskov, J. K. *Appl. Catal., A* **2001**, *222*, 19.

(17) Cattania, M. G.; Parmigiani, F.; Ragaini, V. *Surf. Sci.* **1989**, *211/212*, 1097.

(18) Szmigiel, D.; Bielawa, H.; Kurtz, M.; Hinrichsen, O.; Rosowski, F.; Muhler, M.; Rarog, W.; Jodzis, S.; Kowalczyk, Z.; Znak, L.; Zielinski, J. *J. Catal.* **2002**, *205*, 205.

(19) McClaine, B. C.; Davis, R. J. *J. Catal.* **2002**, *210*, 387.

(20) Bukhtiyarov, V. I.; Slin'ko, M. G. *Russ. Chem. Rev.* **2001**, *70*, 147.

(21) Rosowski, F.; Hornung, A.; Hinrichsen, O.; Herein, D.; Muhler, M.; Ertl, G. *Appl. Catal., A* **1997**, *151*, 443.

(22) Briggs, D.; Seach, M. P. *Practical Surface Analysis*; Wiley: Chichester, U.K., 1992; Vol. 1.

(23) Kuznetsov, L. D.; Dmitrenko, L. M.; Rabina, P. D.; Sokolinsky, Y. A. *Ammonia synthesis*; Khimia: Moscow, 1982 (in Russian).

(24) Anderson, J. R. *Structure of Metallic Catalysts*; Academic Press: London, 1975.

(25) Barr, T. L. *Crit. Rev. Anal. Chem.* **1991**, *22*, 229.

(26) Barr, T. L.; Hoppe, E.; Dugall, T.; Shah P.; Seal S. *J. Electron Spectrosc. Relat. Phenom.* **1999**, *98/99*, 95.

(27) Bukhtiyarov, V. I.; Prosvirin, I. P.; Kvon, R. I. *J. Electron Spectrosc. Relat. Phenom.* **1996**, *77*, 7.

(28) Larichev, Y. V.; Moroz, B. L.; Prosvirin, I. P.; Bukhtiyarov, V. I.; Likholobov, V. A. *Chem. Sustainable Dev.* **2003**, *11*, 155.

(29) Bartzold, R. C. *Surf. Sci.* **1981**, *106*, 243.

(30) Wagner, C. D.; Gale, C. D.; Raymond, R. H. *Anal. Chem.* **1979**, *51*, 466.

(31) Lewis, R. T.; Kelly, M. A. *J. Electron Spectrosc. Relat. Phenom.* **1980**, *20*, 105.

(32) Werthiem, G. K. *Z. Phys. B* **1987**, *66*, 53.

(33) Nefedov, V. I.; Gati, D.; Dzhurinskii, B. F.; Serguhin, N. P.; Salyn, Y. V. *Russ. J. Inorg. Chem.* **1975**, *20*, 2307.

(34) Yang, S. J.; Bates, C. W. *Appl. Phys. Lett.* **1980**, *36*, 675, and literature cited therein.

(35) Ebbinghaus, G.; Simon, A. *Chem. Phys.* **1979**, *43*, 117.

(36) Ayyoob, M.; Hedge, M. S. *Surf. Sci.* **1983**, *133*, 516.

(37) Podgornov, E. A.; Prosvirin, I. P.; Bukhtiyarov, V. I. *J. Mol. Catal. A: Chem.* **2000**, *158*, 337.

(38) Hwang, C. C.; An, K. S.; Park, R. J.; Kim, J. S.; Lee, J. B.; Park, C. Y.; Lee, S. B.; Kimura, A.; Kakizaki, A. *J. Electron Spectrosc. Relat. Phenom.* **1998**, *88*, 733.

(39) Hrbek, J.; Yang, Y. W.; Rodriguez, J. A. *Surf. Sci.* **1993**, *296*, 164.

(40) Tanabe, K. In *Catalysis: Science and Technology*; Anderson, J. R., Boudart, M., Eds.; Springer: Berlin, 1981; Vol. 2, p 231.

(41) Ebbinghaus, G.; Braun, W.; Simon, A.; Berresheim, K. *Phys. Rev. Lett.* **1976**, *37*, 1770.

(42) Aika, K.; Shimazaki, K.; Hattori, Y.; Ohya, A.; Ohshima, S.; Shirota, K.; Ozaki, A. *J. Catal.* **1985**, *92*, 296.

(43) Bates, C. W. *Phys. Rev. Lett.* **1981**, *47*, 204, and literature cited therein.

(44) Shitova, N. B.; Dobrynkin, N. M.; Noskov, A. S.; Prosvirin, I. P.; Bukhtiyarov, V. I.; Kochubei, D. I.; Tsyrul'nikov, P. G.; Shlyapin, D. A. *Kinetica i Kataliz* (*Kinetics & Catalysis*) **2004**, *45*, 414.

(45) Larichev, Y. V.; Prosvirin, I. P.; Shlyapin, D. A.; Shitova, N. B.; Tsyrul'nikov, P. G.; Bukhtiyarov, V. I. *Kinetica i Kataliz* (*Kinetics & Catalysis*) **2005**, *46*, 597.